Schizosaccharomyces pombe protein phosphatase 1 in mitosis, endocytosis and a partnership with Wsh3/Tea4 to control polarised growth

Isabel Alvarez-Tabarés[1,2,*], Agnes Grallert[1], Jose-Miguel Ortiz[2] and Iain M. Hagan[1,‡]

[1]CRUK Cell Division Group, Paterson Institute for Cancer Research, University of Manchester, Wilmslow Road, Manchester, M20 4BX, UK
[2]Departamento de Biología Molecular, Facultad de Medicina, Unidad de Biomedicina-CSIC,Universidad de Cantabria, 39011 Santander, Spain
*Present address: Departamento de Biotecnología Microbiana, Centro Nacional de Biotecnología-CSIC, Campus de Cantoblanco-UAM, 28049 Madrid, Spain
‡Author for correspondence (e-mail: ihagan@picr.man.ac.uk)

Accepted 24 July 2007
Journal of Cell Science 120, 3589-3601 Published by The Company of Biologists 2007
doi:10.1242/jcs.007567

Summary

PP1 holoenzymes are composed of a small number of catalytic subunits and an array of regulatory, targeting, subunits. The *Schizosaccharomyces pombe* genome encodes two highly related catalytic subunits, Dis2 and Sds21. The gene for either protein can be individually deleted, however, simultaneous deletion of both is lethal. We fused enhanced green fluorescent protein (*EGFP*) coding sequences to the 5′ end of the endogenous *sds21*$^+$ and *dis2*$^+$ genes. Dis2.NEGFP accumulated in nuclei, associated with centromeres, foci at cell tips and endocytic vesicles. This actin-dependent endocytosis occurred between nuclei and growing tips and was polarised towards growing tips. When *dis2*$^+$ was present, Sds21.NEGFP was predominantly a nuclear protein, greatly enriched in the nucleolus. When *dis2*$^+$ was deleted, Sds21.NEGFP levels increased and Sds21.NEGFP was then clearly detected at centromeres, endocytic vesicles and cell tips. Dis2.NEGFP was recruited to cell tips by the formin binding, stress pathway scaffold Wsh3 (also known as Tea4). Wsh3/Tea4 modulates polarised tip growth in unperturbed cell cycles and governs polarised growth following osmotic stress. Mutating the PP1 recruiting RVXF motif in Wsh3/Tea4 blocked PP1 binding, altered cell cycle regulated growth to induce branching, induced branching from existing tips in response to stress, and blocked the induction of actin filaments that would otherwise arise from Wsh3/Tea4 overproduction.

Supplementary material available online at
http://jcs.biologists.org/cgi/content/full/120/20/3589/DC1

Key words: Dis2, PP1, *Schizosaccharomyces pombe*, Tea4, Wsh3, Endocytosis

Introduction

Reversible protein phosphorylation is one of the most widespread mechanisms by which eukaryotes modulate the activity of biological pathways. Although the fidelity of this signalling invariably relies upon the reversibility of the reaction, most genomes contain around 20 times fewer Serine/threonine (Ser/Thr) protein phosphatases than Ser/Thr protein kinases (Manning et al., 2002). The diversity amongst these kinases generally arises from the fusion of a particular type of catalytic domain with a distinct series of motifs that impart a unique set of properties to each member of a particular kinase family. By contrast, diversity amongst protein Ser/Thr phosphatases generally arises from the generation of holoenzymes with unique properties via the recruitment of generic catalytic subunits to a range of regulatory subunits at particular locations (Ceulemans et al., 2002). The physico-chemical properties of these catalytic subunits have been used to classify Ser/Thr phosphatases into four major classes; PP1, PP2A, PP2B, PP2C (Ingebritsen and Cohen, 1983). Type 1 protein phosphatases (PP1) have been linked, via the action of more than 50 regulatory subunits, to control events as diverse as cell cycle control and glycolysis (reviewed by Ceulemans and Bollen, 2004). Whereas mammalian cells contain four isoforms of the PP1 catalytic subunit (α, β, γ_1, γ_2 and δ), fission yeast contains two and the budding yeast just one (Ceulemans and Bollen, 2004; Ohkura et al., 1989). The unicellular lifestyle, sophisticated genetics and systematic approaches to study phosphorylation (Ptacek et al., 2005) makes yeasts particularly attractive models for the study of PP1 function (Stark, 1996).

Fission yeast cells grow by actin-mediated cell extension (Hayles and Nurse, 2001; Marks and Hyams, 1985; Mitchison and Nurse, 1985). The point at which this extension occurs is determined by a number of cell polarity determinants that are delivered to the cortex by interphase microtubules (Hagan, 1998; Hayles and Nurse, 2001). The founder member of this class of proteins is the kelch domain protein Tea1 that associates with Mal3, Tip1, Tea2 and Wsh3 (also known as Tea4; hereafter referred to as Wsh3/Tea4) (Browning et al., 2003; Browning et al., 2000; Busch and Brunner, 2004; Mata and Nurse, 1997). Mal3 and Tip1 are the fission yeast homologues of mammalian EB1 and CLIP170, respectively (Beinhauer et al., 1997; Brunner and Nurse, 2000). Tea2 is a kinesin that stabilises microtubules and is required for efficient delivery of Tea1, Tip1 and Mal3 to cell tips (Browning et al., 2003; Browning et al., 2000). Once delivered to cell tips, Tea1 relies upon a Tip-associated CAAX box protein, Mod5, to bind to the cell cortex at the tip (Snaith and Sawin, 2003). It is assumed that the subsequent association of Tea1 with Bud6, For3 and Wsh3/Tea4 promotes actin polymerisation to

maintain polarised, linear growth of the rod shaped cells (Feierbach and Chang, 2001; Feierbach et al., 2004; Glynn et al., 2001; Martin et al., 2005; Tatebe et al., 2005). Wsh3/Tea4 contains a RVXF PP1 binding consensus motif (Meiselbach et al., 2006) and provides a physical and functional link with the stress response signalling cascade, so that cells that lack Wsh3/Tea4 are unable to control cell polarity following stress (Tatebe et al., 2005).

The polarity determinants operate at a second level of polarised growth. Following medial fission, daughter cells grow from the end that existed in the previous cell cycle, while the end that was generated by cytokinesis lies dormant until a discrete point known as new end take off (NETO) when this 'new' end starts to grow (Mitchison and Nurse, 1985). NETO is trigged by the attainment of a critical cell volume and passage through S phase to an ill-defined point within G2 phase. This second level in the polarisation of cell growth also relies upon the cytoskeletal polarity determinants Tea1, Tea3, Bud6 and For3 alongside protein kinases such as Pom1 (Arellano et al., 2002; Bähler and Pringle, 1998; Feierbach and Chang, 2001; Glynn et al., 2001; Mata and Nurse, 1997).

Here we report the distribution of the two PP1 isoforms in fission yeast to new subcellular locations and demonstrate that the recruitment of Dis2 to cell tips by Wsh3/Tea4 is important for the regulation of the microtubule-mediated polarised tip growth.

Results

S. pombe PP1 molecules can tolerate fusion of tags to their N but not C termini

In order to identify the location of Dis2 and Sds2 in the cell, sequences encoding EGFP were fused, in frame, to their genes at their native loci using the 'marker switch approach' (MacIver et al., 2003a). Deletion of both PP1 encoding genes is lethal, whereas deletion of either alone is not (Ohkura et al., 1989). We therefore tested the functionality of each tagged allele by attempting to generate double mutants in which each PP1–tag gene fusion would be the sole source of PP1. An inability to generate such tag-deletion double mutants would indicate that fusion of the tag to the ORF had compromised gene function. *sds21* and *dis2* alleles in which EGFP was fused to the 3′ end of the gene could not act as the sole source of PP1 (data not shown). By contrast, the fusion of a single EGFP molecule and a spacer of three consecutive alanine residues to the N terminus of *dis2*$^+$ and *sds21*$^+$ did not affect the viability, morphology or generation time (data not shown). The actin and microtubule cytoskeletons of these strains were indistinguishable from the relevant *dis2*$^+$ *sds21.Δ* or *dis2.Δ sds21*$^+$ control strains (data not shown).

Dis2 and Sds21 are recruited to distinct sites

Imaging *dis2.NEGFP sds21*$^+$ interphase cells established that Dis2.NEGFP fusion proteins were recruited to the nucleus, a bright spot on the nuclear periphery, numerous cytoplasmic dots at the cell periphery and zones at cell tips (Fig. 1A, supplementary material Movie 1). Double labelling with Hoechst 33342 to identify the hemispherical chromatin region (Toda et al., 1981) confirmed that Dis2.NEGFP gave a general nuclear stain rather than enrichment in a particular sub-domain of the nucleus (Fig. 1B). During mitosis the strong dot at the nuclear periphery was replaced, until anaphase, by up to six spots within the main body of the nucleus (Fig. 1C upper insets, supplementary material Movie 2). During anaphase, a single spot was seen at each end of the separating nuclei to persist as a nuclear peripheral dot in the next cell cycle (Fig. 1C lower insets). Dis2.NEGFP accumulated at the cell equator in early anaphase (Fig. 1A,C green arrow, supplementary material Movie 2).

Centromere association of Dis2

Centromeres associate with the spindle pole body (SPB) throughout interphase. In mitosis they are transiently released before being pulled by microtubules to the two spindle poles.

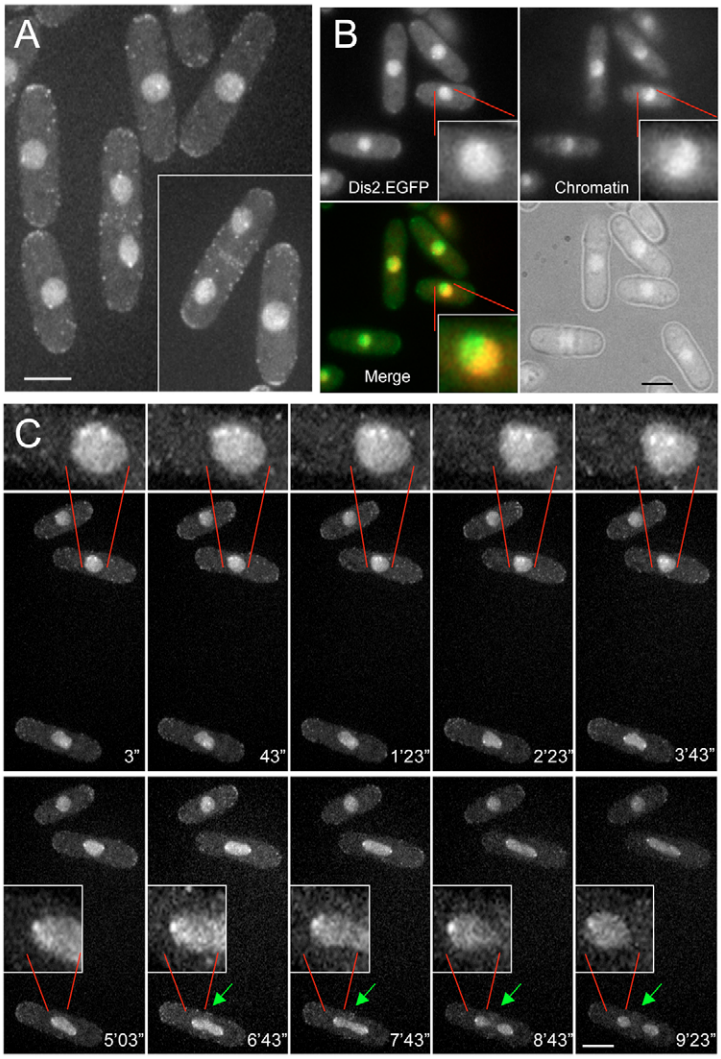

Fig. 1. Dis2.NEGFP accumulates in nuclei, dots within the nucleus and at the cell periphery. *dis2.NEGFP* (IH2908) cells were grown to mid-log phase in EMM2-FS and mounted in EMM2-FS with (B) or without (A,C) 10 μg/ml Hoechst 33342. In A the inset shows Dis2.NEGFP on both sides of a primary septum. In B and C the insets show enlargements of the indicated nuclei. In C the green arrows indicate the accumulation of Dis2.NEGFP in the cytokinetic actin ring during anaphase. See also Movies 1 and 2 in supplementary material. Bars, 5 μm.

In anaphase they re-establish their affiliation with the interphase SPBs (Funabiki et al., 1993). As aspects of Dis2.NEGFP distribution mimic centromere behaviour and PP1 colocalises with kinetochores and centromeric proteins in other systems (Bloecher and Tatchell, 2000; Trinkle-Mulcahy et al., 2003), we imaged the green signal of Dis2.NEGFP alongside red signals arising from Pcp1.RFPC or Cnp1.Cherry to mark SPBs and centromeres, respectively (Fig. 2A-D). We were able to capture images in which the bright Dis2.NEGFP signals formed discrete dots adjacent to the SPB signal (Fig. 2A,B). Rapid movements of the SPB made it a challenge to capture the signal in two distinct fluorescence channels without any movement between the consecutive images. Depolymerisation of the microtubule cytoskeleton with carbendazim (CBZ) to block SPB-mediated nuclear migration (Hagan and Yanagida, 1997) suppressed this movement and enabled us to establish that, although the Pcp1.RFPC and Dis2.NEGFP signals were close, they very rarely overlapped, indicating that the two fluorochromes were associated with distinct structures (Fig. 2B).

The association of Dis2.NEGFP signals with SPBs was exceptionally rare from the commitment to mitosis until anaphase when they were seen just inside the nucleus adjacent to the SPB (data not shown). By contrast, the centromere marker overlapped with the Dis2 signal at all stages of the cell cycle (Fig. 2C,D). Chromatin immunoprecipitation (ChIP) established that Dis2.NPk associated with centromeric sequences. Sequences corresponding to the central core non-repetitive domains of the centromere that promote the formation of the kinetochore were enriched in immunoprecipitates whereas those in the flanking outer or inner repeats were not (Fig. 2E). Association with protein complexes in the central region is consistent with the inability of Dis2.NEGFP to colocalise with centromeres when an inner centromere component that is required for the loading of the centromere-specific histone H3 variant CenpA to the centromere, Mis6 is defective (Saitoh et al., 1997; Takahashi et al., 2000). *mis6.302 dis2.NEGFP pcp1.RFPC* cells were incubated at 36°C for 6 hours. Almost three-quarters of interphase cells (73%) did not have any punctate signals that would correspond to Dis2.NEGFP at centromeres near the SPB or dispersed throughout the nucleoplasm (data not shown). Thus, not only do the Dis2.NEGFP foci that associate with interphase SPBs and strong mitotic Dis2.NEGFP dots colocalise with centromeres, but they are disrupted upon disruption of centromere function. We conclude that these structures represent Dis2.NEGFP recruitment to centromeres.

Distribution of Sds21.NEGFP

Signals from the Sds21.NEGFP differed from those from Dis2.NEGFP in three respects (Fig. 3A). First, although Sds21.NEGFP was a nuclear protein it was enriched in the non-Hoechst 33342 staining nucleolus (Toda et al., 1981). Second, the Sds21.NEGFP nuclear signal was considerably fainter than that from Dis2.NEGFP (supplementary material Fig. S2B). Third, *sds21.NEGFP* expressing strains did not show any punctate signals in the cytoplasm or give the characteristic spot on the nuclear periphery that results from centromere association (Fig. 3A).

Sds21.NEGFP associates with structures that recruit Dis2.NEGFP in *dis2.Δ* cells

Although Sds21.NEGFP and Dis2.NEGFP have strikingly different distributions, cells that lack either molecule are viable and, yet, those that lack both are dead (Ohkura et al., 1989), suggesting either that the association of Dis2.NEGFP with some of the structures is not essential, or that the removal of one isoform enables the other to substitute and assume

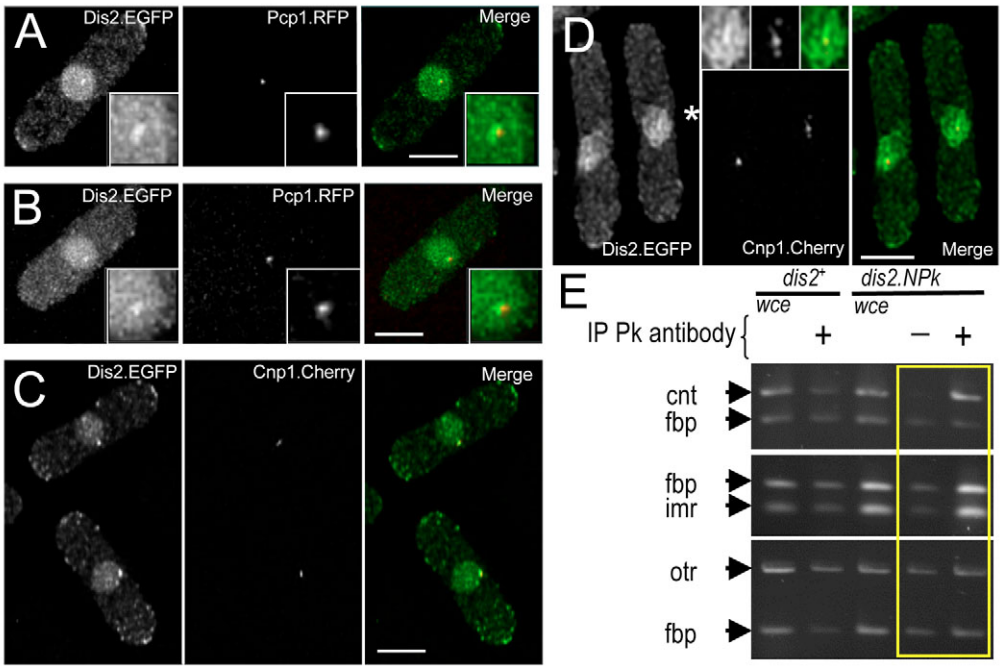

Fig. 2. Dis2.NEGFP associates with centromeres. *dis2.NEGFP pcp1.RFPC* (IH2731; A,B) and *dis2.NEGFP cnp1.Cherry* (IH5283; C,D) cells were processed as for Fig. 1 with the exception that DMSO or DMSO containing CBZ at a final concentration of 25 μg/ml were included in the culture medium for imaging in A and B, respectively. (A,B) The Dis2.NEGFP signal does not colocalise with the Pcp1.RFPC signal of interphase cells. (C,D) The Dis2.NEGFP signal colocalises with the Cnp1.Cherry signal of interphase (C) and mitotic (D) cells. Inset in D shows enlargement of the nucleus marked with the asterisk. (E) For ChIP analysis whole cell extracts (wce) were prepared from the indicated strains for precipitation with magnetic beads to which either no antibody (–) or a rabbit antibody that recognised the Pk epitope (+) had been covalently attached. There was a clear enrichment of the signal arising from PCR with primers to the central but no other sequences in immunoprecipitates from *dis2.NPk* (lane 5), but not when antibodies were not conjugated to the beads (lane 4) or the strain did not contain the tagged *dis2*$^{+}$ gene (lane 2). Bars, 5 μm.

functions that were normally executed by the missing phosphatase. We therefore examined the distribution of each phosphatase in strains from which the second isoform had been deleted (Fig. 3B,C). Dis2.NEGFP distribution and signal intensity did not change when *sds21*$^{+}$ was deleted (Fig. 3C,E). Significantly, there was no enhancement of the staining of the nucleolar region that might be expected if Dis2 were now to be recruited to sites formerly occupied by Sds21 (Fig. 3C,E). By contrast, deletion of *dis2*$^{+}$ from *sds21.NEGFP* led to the incorporation of Sds21.NEGFP into all of the locations that would otherwise have been occupied by Dis2, with the exception of chromatin and the staining around the cell equator during division (Fig. 3B and supplementary material Fig. S1). Furthermore, when we marked *sds21.NEGFP dis2*$^{+}$ cells by transient immersion in red fluorescent lectin before imaging them alongside *sds21.NEGFP dis2.Δ* we found that deletion of *dis2*$^{+}$ prompted an increase in the intensity of the Sds21.NEGFP signal (Fig. 3D). Western blotting established that this increase in signal was due to an increase in protein level (Fig. 3F and supplementary material Fig. S2). Such an increase in Sds21 levels and recruitment to new sites suggested that Sds21 is competent to associate with targeting molecules that have a much greater affinity for Dis2 when Dis2 is present.

Two classes of cytoplasmic Dis2.NEGFP foci

Treatment with the microtubule depolymerising drug carbendazim (CBZ) altered Dis2.NEGFP distribution (Fig. 4, supplementary material Movies 3, 4). The inclusion of *nmt81.GFP.atb2* expressing cells (asterisks Fig. 4, supplementary material Movies 3, 4) (Garcia et al., 2001) alongside *dis2.NEGFP* cells enabled us to establish that microtubules had been destroyed by CBZ treatment because no discrete GFP signals were visible in the *nmt81GFP.atb2* cells (Fig. 4C,D). Time-lapse series following microtubule depolymerisation revealed that cytoplasmic Dis2.NEGFP foci could be divided into two distinct subpopulations that differed in response to CBZ. Slightly larger foci that formed a cap at the cell tips (inset in Fig. 4B, blue brackets in Movies 1 and 3 in supplementary material) were lost following microtubule depolymerisation (inset Fig. 4D, supplementary material Movie 4), whereas the more numerous dots that were seen further back from the tips throughout the cytoplasm were unaffected by microtubule disruption (Fig. 4, compare insets of B and D, supplementary material Movies 3, 4).

Small cytoplasmic Dis2.NEGFP foci and endocytosis

Imaging single focal planes revealed that the small foci of Dis2.NEGFP appeared at the cortex and moved a short distance into the cytoplasm before disappearing again (supplementary material Movie 1, yellow brackets and arrows). Continual imaging of three consecutive z sections of 0.2 μm over short intervals established that the disappearance of dots reflected a genuine dispersal or disassociation of Dis2.NEGFP from these structures or dissolution of the structures rather than movement out of a particular focal plane (supplementary material Movie 5, data not shown). Generating kymographs by compressing the region delineated by green bars in Fig. 5A to give a single slice and then lining up consecutive slices one after another, established that dots persisted for an average of 7.9 seconds (a total of 61 dots monitored).

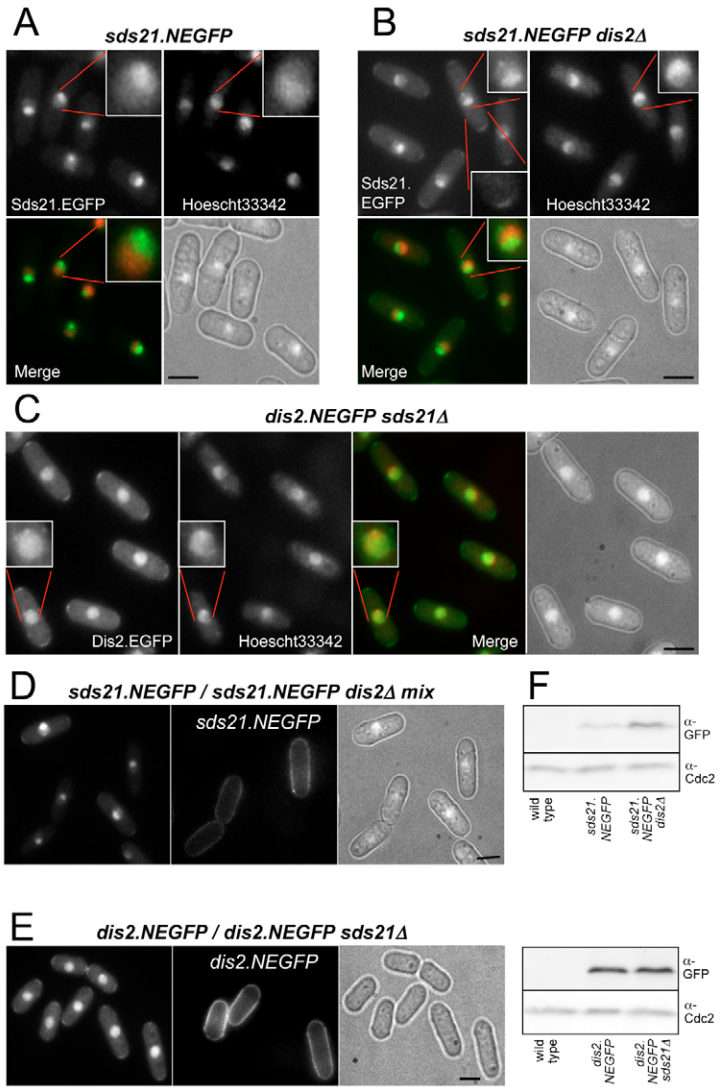

Fig. 3. Sds21.NEGFP accumulates in nuclei, dots within the nucleus and at the cell periphery. Cells of the indicated strains were grown as for Fig. 1 with (A-C) or without (D,E) 10 μg/ml Hoechst 33342. In D and E the strains indicated in the central panel were transiently exposed to TRITC-lectin before being mixed and mounted with the deletion strain. (A,B) Sds21.NEGFP accumulates in nucleoli of *dis2*$^{+}$ cells (IH2352) and is recruited to all sites normally occupied by Dis2.NEGFP when the *dis2*$^{+}$ gene has been deleted (IH2635). (C) The distribution of Dis2.NEGFP is not affected by deletion of *sds21*$^{+}$(IH2090). (D) Imaging *sds21.NEGFP* cells that have been dipped in red lectin (central micrograph) alongside *sds21.NEGFP dis2.Δ* cells shows an increase in the intensity of the Sds21.NEGFP signal upon deletion of *dis2*$^{+}$. (E) Imaging *dis2.NEGFP* cells that have been dipped in red lectin (central micrograph) alongside *dis2.NEGFP sds21.Δ* cells shows no increase in the intensity of the Dis2.NEGFP signal upon deletion of *sds21*$^{+}$. (F) Western blotting with antibodies to GFP establishes that the increase in Sds21.NEGFP signal intensity in *dis2.Δ* arises from an increase in protein levels. A-E. Bar, 5 μm.

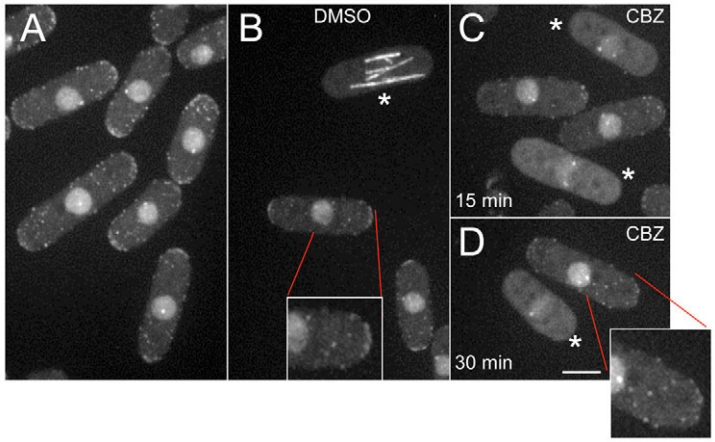

Fig. 4. Dis2.NEGFP recruitment to cell tips requires microtubules. *dis2.NEGFP* (IH2908; A) and a mix of *dis2.NEGFP* (IH2908) and *nmt81.GFP.atb2* (IH1741) cells (B-D) were processed as for Fig. 1 with the exception that DMSO containing CBZ, to a final concentration of 25 μg/ml, was included in the culture medium for mounting in C and D and an equivalent amount of DMSO was added to the culture in B. Whereas Dis2.NEGFP distribution was not affected by the addition of DMSO (B), disruption of the microtubule cytoskeleton (verified by the lack of any microtubule signals in the control *nmt81.GFP.atb2* cells, asterisks) abolished the association of Dis2.NEGFP with cell tips (compare inset in B to that in D). See also Movies 3 and 4 in supplementary material. The Dis2.NEGFP dots that are seen away from the cell tip were not affected by microtubule depolymerisation. Bar, 5 μm.

Inward migration of spots is reminiscent of that of endocytic proteins such as Sla2, Myo1 and Arp2/3 (Castagnetti et al., 2005; Sirotkin et al., 2005). We therefore fused sequences encoding the red fluorescent protein 'Cherry' (Shaner et al., 2004) to the 3′ end of the *end4*$^{+}$ (also known as *sla2*$^{+}$) gene that is required for endocytosis (Iwaki et al., 2004) and recorded consecutive Sla2.Cherry and Dis2.NEGFP signals from the same cell (Fig. 5B). The strong accordance between the two signals is consistent with the two proteins associating with each other or with a common structure. Moreover, efficient movement of Dis2.NEGFP foci relied upon Sla2 function because 67% of Dis2.NEGFP foci (*n*=239) appeared at the cell cortex, but failed to migrate towards the cell centre, in the temperature sensitive *sla2.Δ* background at 33°C [Fig. 5C; 100% of foci (*n*=221) migrate towards the cell centre before disappearing in *sla2*$^{+}$ cells; data not shown]. Furthermore, attempts to combine *sla2.Δ* with the

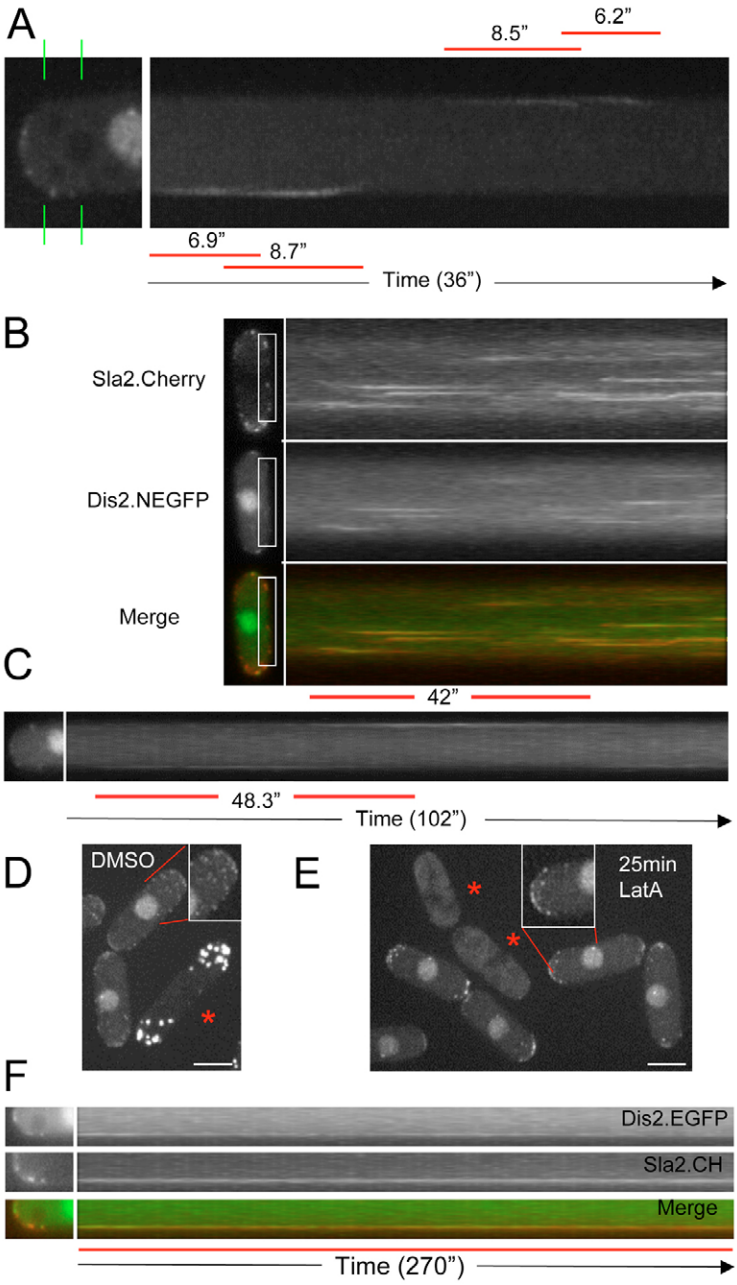

Fig. 5. Dis2.NEGFP in endocytosis. *dis2.NEGFP* (IH2908; A), *dis2.NEGFP sla2.Cherry* (IH5205; B), *dis2.NEGFP sla2.Δ* (IH4722; C), a mix of *dis2.NEGFP* (IH2908) and *crn1.GFP* (IH3528) cells (D,E) and a mix of *dis2.NEGFP sla2.Cherry* (IH5205) and *act1.GFP* (IH4266) cells (F) were processed as for Fig. 1 with the exception that DMSO containing Lat A, to a final concentration of 50 μM, was included in the culture medium for mounting in E and F and an equivalent amount of DMSO added to the culture in D. (A) Kymograph of the area between the green lines shows the internalisation movement of Dis2.NEGFP. (B) Kymograph of the area in the rectangles shows the colocalisation of Dis2.NEGFP and Sla2.Cherry. Note that Sla2.Cherry signal appears at the cell cortex before Dis2.NEGFP (C) Kymograph showing that the internalisation of Dis2.NEGFP is avoided in *sla2.Δ* cells grown at 33°C. (D,E) Whereas Dis2.NEGFP distribution was not affected by the addition of DMSO (D), disruption of the actin cytoskeleton (verified by the lack of any Crn1.GFP signals in the control *crn1.GFP* cells – asterisks) severely reduced the number of Dis2.NEGFP dots seen away from the cell tip, but did not affect the association of Dis2.NEGFP with cell tips (compare inset in D and E). Bars, 5 μm. (F) Kymograph showing that internalisation of Dis2.NEGFP and Sla2.CH foci was abolished by depolymerisation of the F-actin cytoskeleton.

dis2.11 mutant failed, indicating that the presence of the two mutations in the same cell conferred synthetic lethality (data not shown). We conclude that the small dots are likely to represent an association with endocytic vesicles to regulate some aspects of early stages of endocytosis. We refer to these dots as Dis2.NEGFP endocytic associated foci (DEAF).

As actin plays a key role in endocytosis, mixed cultures of *dis2.NEGFP* or *dis2.NEGFP sla2.Cherry* and *crn1.GFP* (Pelham, Jr and Chang, 2001) were treated with latrunculin A (Lat A) to depolymerise F-actin. This treatment abolished the *crn1.GFP* signal, indicating that it effectively removed the F-actin cytoskeleton (asterisk in Fig. 5E). In the neighbouring cells Lat A treatment froze the migration of the Dis2.NEGFP and Sla2.Cherry DEAFs at the cortex and they failed to migrate into the cytoplasm (Fig. 5E,F). The distribution of the tip-associated Dis2.NEGFP foci was unaffected by disruption of the actin cytoskeleton. However, fewer DEAFs than in unperturbed cells appeared throughout the cytoplasm and now localised in the cell tip region (insets in Fig. 5D,E).

Dis2.NEGFP foci and cell polarity

The disappearance of foci from the cell tips upon the disruption of the microtubule cytoskeleton (Fig. 4D, supplementary material Movie 4) prompted us to investigate the relationship between this population of Dis2.NEGFP and polarised tip growth. Staining cells with fluorescent lectin to stain the cell wall can differentiate between growing and non-growing tips if cells are returned to the cell culture to resume growth and generate non-fluorescent, freshly grown zones (May and Mitchison, 1986). It can therefore be used to stage cells relative to the NETO transition in G2 phase (Mitchison and Nurse, 1985). Transient lectin staining and live cell imaging established that Dis2 associated with cell tips irrespective of whether they were growing or not (Fig. 6A,B). Furthermore, both ends of cells in which cell cycle progression had been arrested before NETO, with the *cdc10.129* mutation, recruited Dis2.NEGFP to the same degree as those arrested at the G2-M boundary, after NETO, with the *cdc25.22* mutation (Fig. 6C,D).

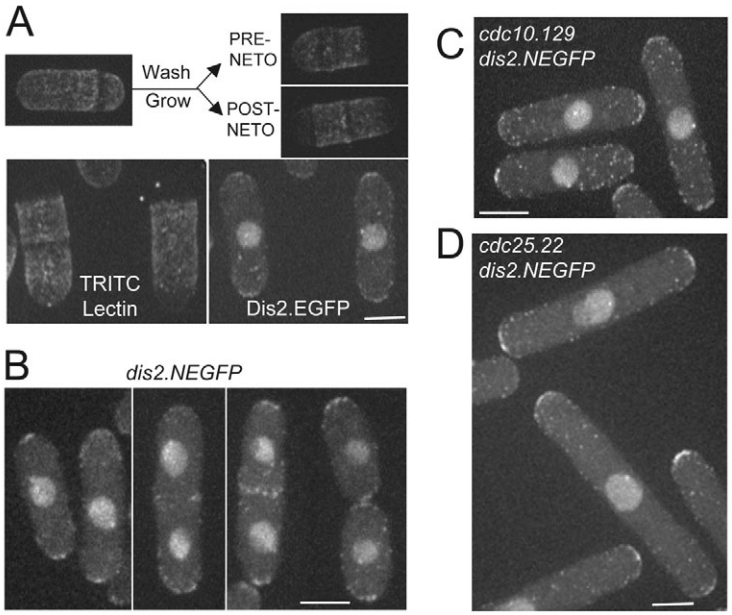

Fig. 6. Dis2.NEGFP associates with both growing and non-growing tips. *dis2.NEGFP* (IH2908; A,B), *dis2.NEGFP cdc10.129* (IH2345; C) and *dis2.NEGFP cdc25.22* (IH2356; D) cells were processed as for Fig. 1. (A) Prior to mounting, *dis2.NEGFP* cells were re-suspended in TRITC-lectin so that the entire cell surface became fluorescent. Washing this lectin out by repeated changes of medium and subsequent growth resulted in dark non-stained tips, identifying those tips that were actively growing and those that were not (stained tips). (B) Dis2.NEGFP foci associated with the cell tips during interphase, mitosis and immediately after cytokinesis. Note the lower Dis2.NEGFP signal intensity at the tips of mitotic cells. (C,D) Dis2.NEGFP associated with both cell tips in cells that are arrested before NETO at START (C) and after NETO at the G2-M boundary (D). Bars, 5 μm.

Dis2.NEGFP recruitment to cell tips requires Tea1

Because the dependence of the tip association of Dis2.NEGFP upon an intact microtubule cytoskeleton mirrors that of polarity determinants such as Tea1, we assessed the impact of abolition of the function of polarity determinants upon Dis2.NEGFP distribution. Dis2.NEGFP associated with the tips of *tea3.Δ*, *pom1.Δ* and *bud6.Δ* cells (Fig. 7A-C) but failed to form caps at the tips of *tea1.Δ*, *mal3.Δ*, *tip1.Δ* and *tea2.1* cells (Fig. 7D-G). As microtubules do not reach the tips of *mal3.Δ*, *tip1.Δ* and *tea2.1* cells (Beinhauer et al., 1997; Browning et al., 1998; Brunner and Nurse, 2000; Verde et al., 1995), the lack of a Dis2.NEGFP cap at the tips of these cells could simply be due to the inability of microtubules to reach these tips. By contrast, microtubules often fail to stop elongating when they reach the tips of *tea1.Δ* cells (Mata and Nurse, 1997) raising the possibility that it is simply the incorrect behaviour of microtubules at cell tips that affects Dis2.NEGFP association with cell tips. We therefore examined Dis2.NEGFP distribution in *peg1.1* mutants in which the deficiency in CLASP function compromises the termination of microtubules at cell tips so that they also curl around cell tips without affecting Tea1 recruitment (Grallert et al., 2006). Dis2.NEGFP association with cell tips was normal (data not shown). We therefore conclude that Tea1 function is required for the association of Dis2.NEGFP foci with cell tips to form the cap-like structure that is typical of wild-type cells.

The Tea1-related morphogenesis system controls the polarity of endocytosis in *S. pombe*

DEAFs were distributed between cell tips and either side of wild-type nuclei (Fig. 1A, Fig. 8B). Whereas there was a moderate bias towards one end of wild-type cells (presumably the old end), there was a striking polarisation of DEAFs in *cdc10.129* cells that failed to enter the cell cycle and so arrested before NETO (Fig. 6C, Fig. 8B). Strikingly, DEAFs were greatly enriched on the old, growing end of *tea1.Δ* cells (Fig. 7E, Fig. 8). Such hyper-polarisation was not seen in *tea3.Δ*, *bud6.Δ*, *mal3.Δ* or *tea2.1*, although a slight enrichment on one side was observed in *pom1.Δ* and *tip1.Δ*.

Dis2.NEGFP is recruited to cell tips via the RVXF motif of Wsh3/Tea4

Budding yeast PP1, Glc7, is recruited to bud tips by the conserved Bud14 protein (Knaus et al., 2005). The

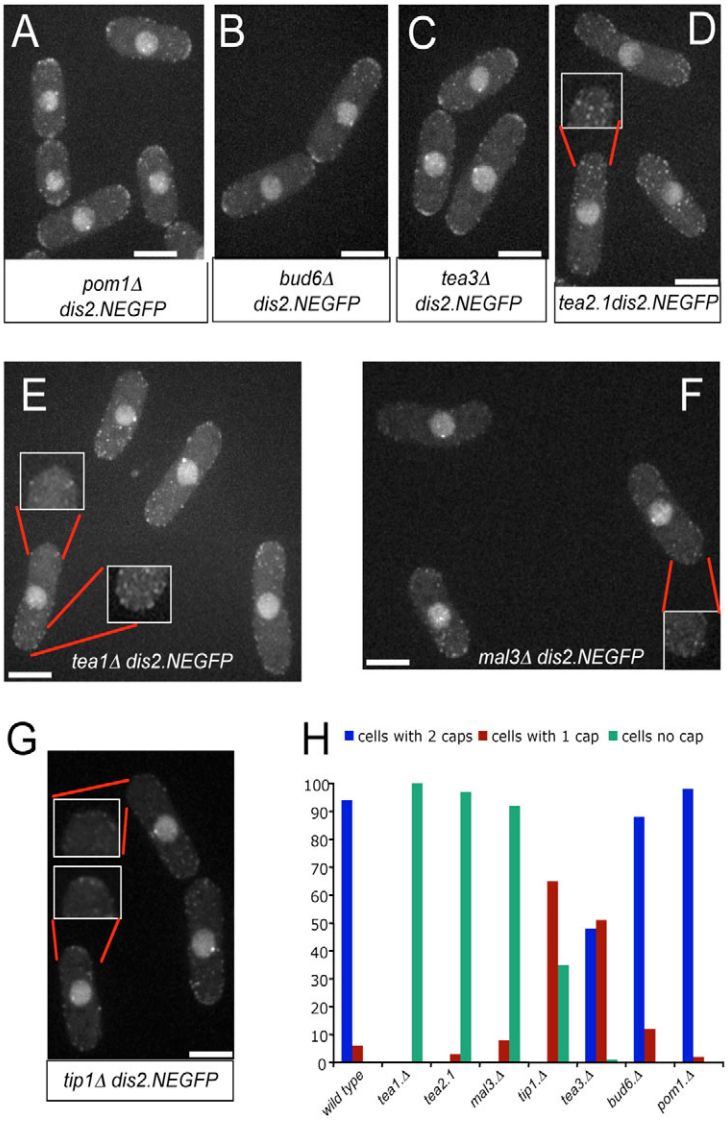

Fig. 7. Abolishing Tea1, Tea2 and Mal3 function abolishes Dis2.NEGFP tip association. Cells of the indicated strains were processed as described for Fig. 1. (A-C) Deletion of *pom1*$^{+}$(IH2349; A), *bud6*$^{+}$ (IH3092; B) or *tea3*$^{+}$ (IH3202; C) did not affect Dis2.NEGFP association with the cell tips. (D-G) Deletion of *tea1*$^{+}$ (IH3201; E), *mal3*$^{+}$ (IH3155; F) or *tip1*$^{+}$ (IH3757; G), and the presence of *tea2.1* (IH2859) grown at 36°C (D) abolished the association of Dis2.NEGFP with cell tips. (H) Quantification of Dis2.NEGFP cap formation. Bars, 5 μm.

fission yeast homologue, Wsh3/Tea4, contains the PP1 binding consensus sequence RVXF (Knaus et al., 2005; Meiselbach et al., 2006), binds Tea1 and the formin For3 at cell tips, and is required to maintain cell polarity during unperturbed cell cycles and following osmotic stress (Martin et al., 2005; Tatebe et al., 2005). Imaging *dis2.NEGFP wsh3*$^{+}$ cells that had been labelled with red lectin alongside unlabelled *dis2.NEGFP wsh3.Δ* cells revealed a cap of Dis2.NEGFP fluorescence in the *wsh3*$^{+}$ but not *wsh3.Δ* background (Fig. 9A, supplementary material Movie 5). Depolymerisation of microtubules abolished the fluorescent cap in both backgrounds (Fig. 9A right panel). The colocalisation of Dis2 and Wsh3/Tea4 at cell tips and the ability to co-immunoprecipitate Dis2.NEGFP with epitope-tagged Wsh3 supported the prediction that Dis2 is recruited to cell tips by Wsh3/Tea4 (Fig. 9B, Fig. 10A, supplementary material Movie 6). Mutation of amino acids 223 and 225 of Wsh3/Tea4 (the V and F residues of the RVXF motif, respectively) to alanine blocked both the ability to co-immunoprecipitate Dis2 with Wsh3/Tea4 and the recruitment of Dis2.NEGFP to tips (Fig. 10A,B and supplementary material Fig. S3) indicating that Wsh3/Tea4 mirrors the relationship between Glc7 and Bud14 in recruiting Dis2.NEGFP to cell tips. Dis2.NEGFP generally associated with Wsh3.C2tdTom foci after they reached the cell tips, however, occasional foci did transiently associate with Wsh3/Tea4 foci along the cell cortex (see supplementary material Fig. S4). Dis2.NEGFP association with Wsh3/Tea4 foci at either the tip or the general cortex was dynamic as the signal intensity at individual foci often oscillated (see inset in Fig. 9B) or faded completely while the intensity of the Wsh3.C2tdTom signals maintained a steady signal (supplementary material Fig. S4).

Dis2 regulates the polarity of cell tip growth and actin polymerisation at cell tips

To address the significance of the recruitment of PP1 to cell tips by Wsh3/Tea4, we investigated whether PP1 docking was critical for the recruitment of this polarity determinant itself to cell tips. We did this in a *wsh3.Δ* background by expressing *wsh3*$^{+}$, *wsh3.V223A* or *wsh3.F225A* genes in which sequences encoding three Pk epitope tags had been inserted, in frame at the C terminus. Wsh3.PkC was recruited to cell tips irrespective of whether it bound Dis2 or not (Fig. 10C). We next addressed the critical role executed by Wsh3/Tea4 in maintaining polarised growth following osmotic stress (Tatebe et al., 2005). We induced varying levels of *wsh3*$^{+}$, *wsh3.V223A* or *wsh3.F225A* expression from the thiamine repressible *nmt41* promoter in *wsh3.Δ* cells by the inclusion of increasing levels of the repressor thiamine in the medium. 20 μM thiamine represses *wsh3*$^{+}$ production to such a degree that no *wsh3*$^{+}$ is detectable at the cell tips (Fig. 10B). Scoring cell morphogenesis 3 hours after induction of osmotic stress established that expression of the wild-type, but not either mutant gene suppressed the morphological defects arising from stressing these *wsh3.Δ* cells (Fig. 10D). The repeated initiation of growth of the old cell end following mitosis in the septation-defective mutant *cdc11.132*, accentuates defects in polarised tip growth that accompany cell cycle progression of *wsh3.Δ* cells (Fig. 10E) (Martin et al., 2005). We therefore compared the morphology of *cdc11.132 wsh3.Δ* cells expressing *wsh3*$^{+}$, *wsh3.V223A* or *wsh3.F225A* and found that the wild-type but neither mutant gene suppressed the morphological defects of *wsh3.Δ cdc11.132* cells (Fig. 10E).

Wsh3/Tea4 binds to the polarity determinant Tea1 and is required to ensure the recruitment of Tea1 to the non-growing tip (Fig. 10F) (Martin et al., 2005). Given the clear requirement for PP1 recruitment to cell tips by Wsh3/Tea4 to control polarity (Fig. 10D,E), we investigated whether it was required for Wsh3/Tea4 to promote Tea1 recruitment to both cell tips. To this end we induced *wsh3*$^{+}$, *wsh3.V223A* or *wsh3.F225A* in

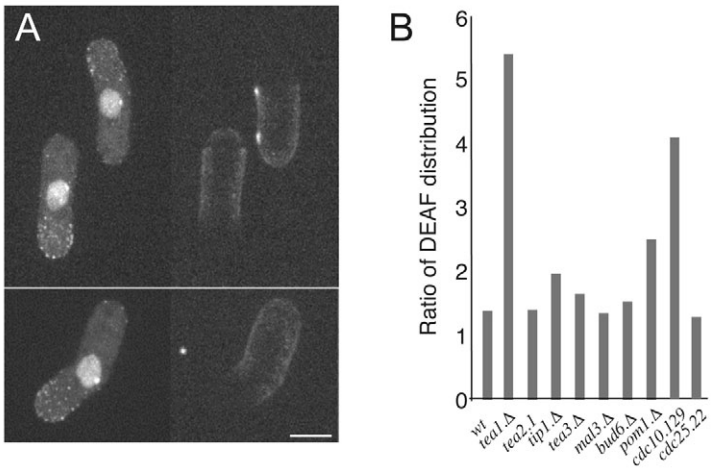

Fig. 8. Transit through NETO and Tea1 function control DEAF distribution. (A) *dis2.NEGFP tea1Δ* cells (IH3210) were processed as in Fig. 6A. Deletion of *tea1*$^{+}$ resulted in a polarised distribution of DEAFs towards the tip, at which new cell wall had been added above the TRITC-lectin coating, indicating that it was the growing tip. Bar, 5 μm. (B) Quantification of DEAF distribution in the indicated strains shows that Tea1 is required to ensure that endocytosis occurs to a similar degree on both sides of the interphase nucleus. The figures on the *y* axis are a ratio of the number of dots seen on one side of the nucleus against those on the other.

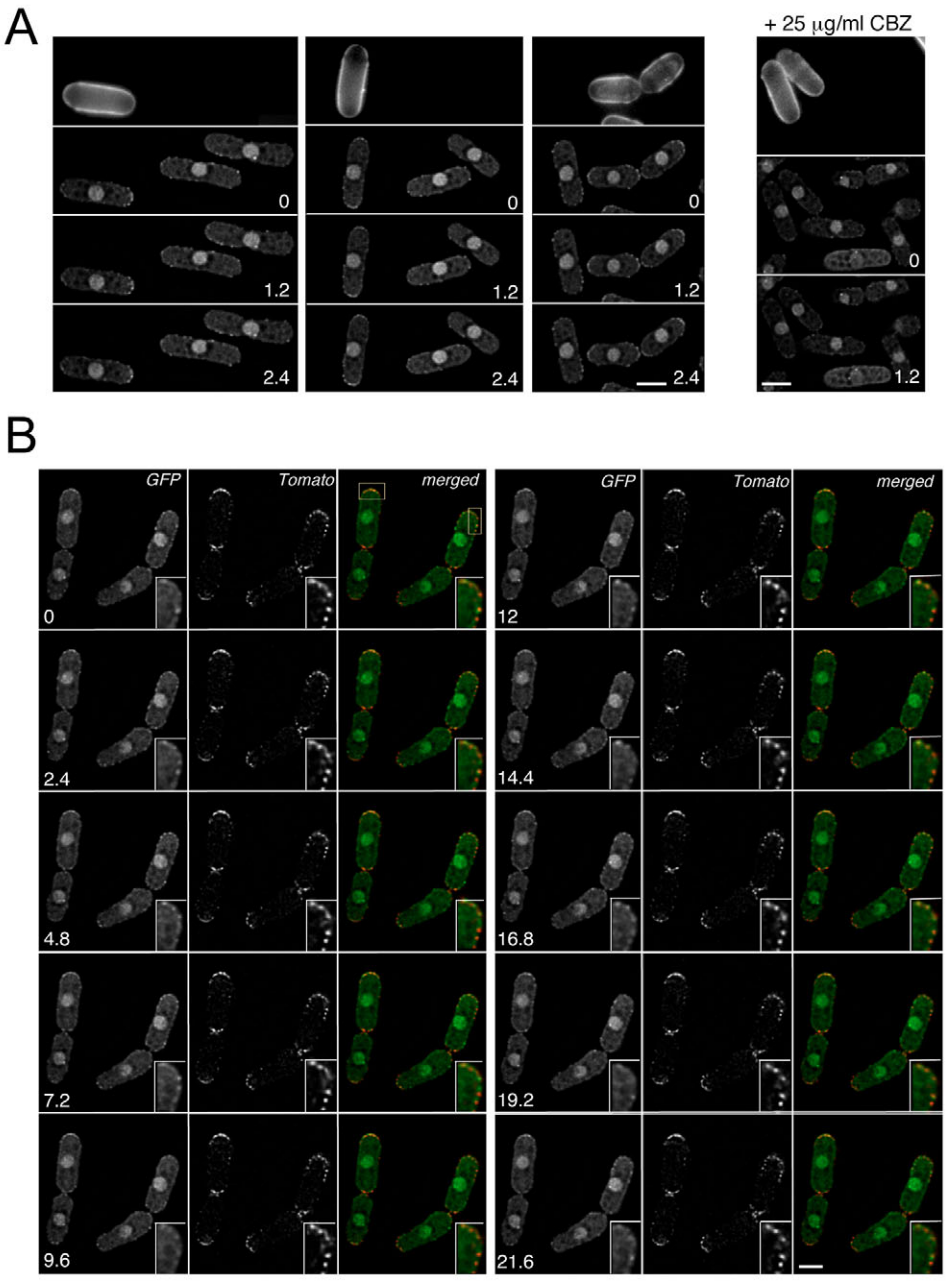

Fig. 9. Wsh3/Tea4 recruits Dis2.NEGFP to cell tips. (A) *dis2.NEGFP wsh3*$^{+}$ (IH2089) cells were dipped in red lectin and mounted alongside *dis2.NEGFP wsh3.Δ* (IH5722) cells. Continuous imaging of GFP fluorescence in three consecutive z slices (compressed into a single maximum projection) showed that the Dis2.NEGFP cap structure seen at the end of *dis2.NEGFP wsh3*$^{+}$ cells was absent when *wsh3*$^{+}$ was deleted (three left panels, see Movie 5 in supplementary material). Depolymerisation of microtubules by the addition of 25 μg/ml CBZ abolished Dis2.NEGFP cap signals in both the *wsh3*$^{+}$ and the *wsh3.Δ* backgrounds (right panel). (B) Consecutive green and red images of *dis2.NEGFP wsh3.C2tdTom* (IH5726) cells were continuously taken in three consecutive z stacks to reveal the dynamics of the association of Dis2.NEGFP with Wsh3.C2tdTom at cell tips. See Movie 6 in supplementary material. Bars, 5 μm.

a *wsh3.Δ tea1.pkGFP* background. Tea1.PkGFP was recruited to both cell tips irrespective of the ability of Wsh3 to recruit Dis2.NEGFP. Thus, the morphological defects arising from mutation of the PP1 binding sites in Wsh3/Tea4 are not a consequence of altered Tea1 recruitment.

In addition to binding Tea1, Wsh3/Tea4 binds to the formin For3 (Martin et al., 2005). Over production of Wsh3/Tea4 promotes the polymerisation of actin to form prominent F-actin cables and alters cell morphology [Fig. 10B, 20 hours, see supplementary material Fig. S2 for levels of expression, Fig. 10G (Martin et al., 2005)]. Significantly, whereas high levels of expression of *wsh3*$^{+}$ induced morphological defects and

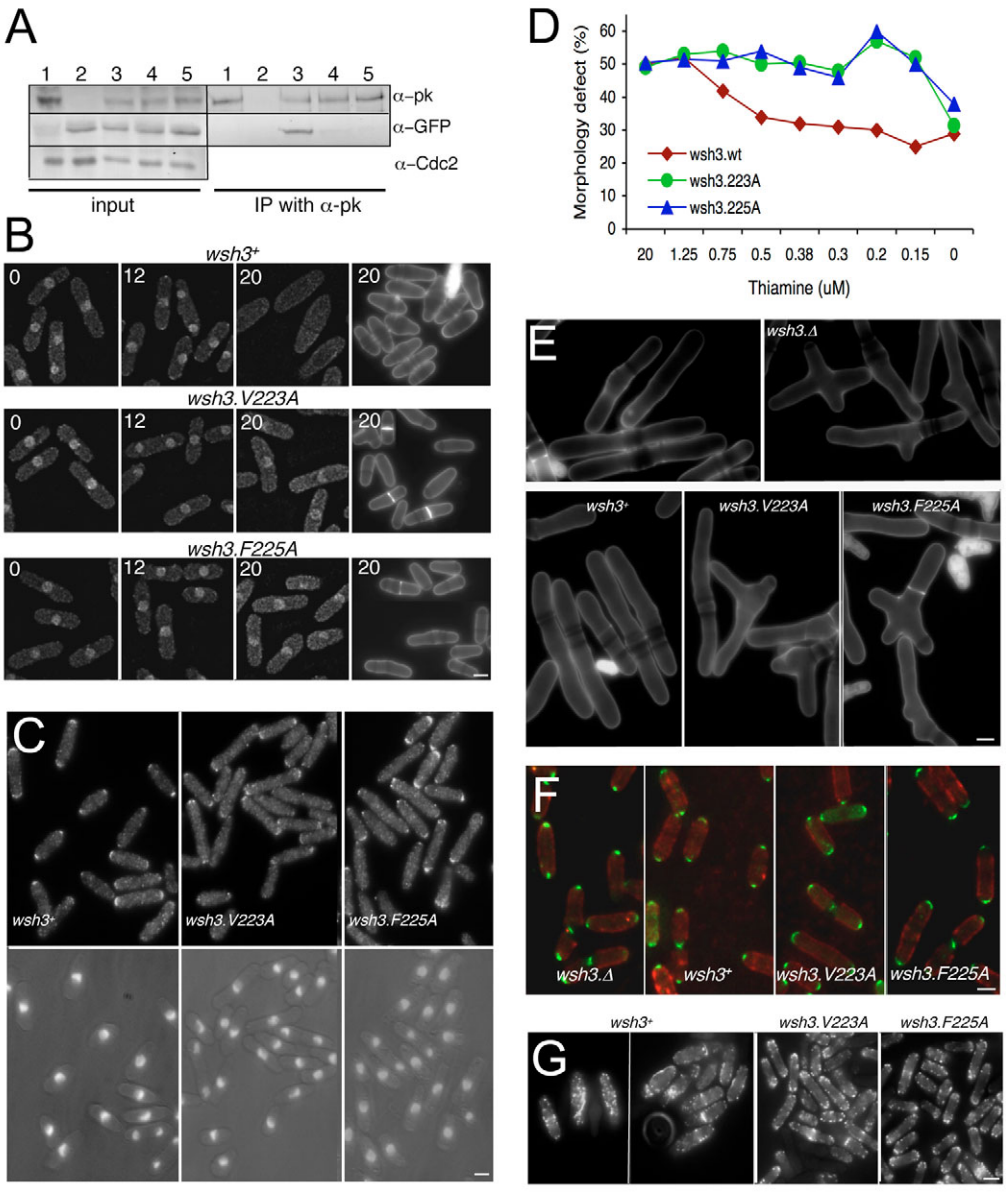

Fig. 10. Recruitment of PP1 to cell tips by Wsh3/Tea4 modulates cell polarity without affecting the recruitment of Wsh3/Tea4 or Tea1. (A) Epitope-tagged *wsh3* genes were induced by derepression of a *leu1::nmt41wsh3.PkCX* transgene in a *wsh3.Δ* background. Extracts were prepared and Pk immunoprecipitates were isolated and blotted with antibodies to recognise the Pk or GFP epitopes. Lane 1: *wsh3.Δ leu1::nmt41wsh3.PkC dis2*$^{+}$(IH5740); 2: *wsh3.Δ leu1*$^{+}$ *dis2.NEGFP* (IH5722); 3: *wsh3.Δ leu1::nmt41wsh3.PkC dis2.NEGFP* (IH5742); 4: *wsh3.Δ leu1::nmt41wsh3.PkC.V223A dis2.NEGFP* (IH5743); 5: *wsh3.Δ leu1::nmt41wsh3.PkC.F225A dis2.NEGFP* (IH5744). (B) *wsh3*$^{+}$, *wsh3.V223A* or *wsh3.F225A* genes were integrated under the control of the *nmt41* promoter at the *leu1* locus. Cells were grown to early log phase in the presence of 20 μM thiamine to repress the expression of the transgene. At time 0 all three cultures were then washed three times in thiamine-free medium to relieve the repression of the transgenes. Cells were then imaged over the indicated time frames after induction to identify Dis2.NEGFP (three left panels) and stained with calcofluor white 20 hours after induction (right panel). Dis2.NEGFP failed to associate with cell tips of any strain when the expression was fully repressed at time 0. Induction of wild-type *wsh3*$^{+}$ gene for 12 hours resulted in recruitment of Dis2.NEGFP to cell tips, whereas similar induction of Wsh3.V223A and Wsh3.F225A did not. The enhanced protein levels 20 hours after induction (see supplementary material Fig. S3) led to complete delocalisation of Dis2.NEGFP and alteration of cell morphology. This enhanced induction of Wsh3 sequestered Dis2.NEGFP away from the nucleus. No adverse effects upon cell morphology or Dis2.NEGFP distribution were apparent when either mutant allele was induced for 20 hours despite the fact that the mutant proteins accumulated to the same degree as the wild type Wsh3 molecules (see supplementary material Fig. S3). (C) Anti-Pk immunofluorescence of cells in which Pk-tagged wild-type or mutant Wsh3 had been induced for 12 hours in *leu1::nmt41wsh3.PkCX wsh3.Δ* (IH 5742, 5743, 5744) cells. (D) *wsh3.Δ leu1::nmt41wsh3.X* cells (IH 5737, 5738, 5739) were grown in the presence of the indicated levels of thiamine, subjected to osmotic shock by the addition of an equal volume of pre-warmed medium containing 2.4 M sorbitol and the proportion of cells with morphological defects was scored 3 hours later. (E) The temperature of *cdc11.132* (IH127) and *cdc11.132 wsh3.Δ* (IH5755) (upper panel) *cdc11.132 wsh3.Δ leu1::nmt41wsh3.X* (IH5761, 5762, 5763; lower panels) cultures was shifted to 36°C in the presence of 0.15 μM thiamine to induce the expression of Wsh3 proteins. (F) *wsh3.Δ tea1.PkGFP* (IH5751; left panel), or *wsh3.Δ tea1.PkGFP leu1::nmt41wsh3.X* (IH5752, 5753, 5754; remaining panels) cells 12 hours after induction of transgene expression. (G) Rhodamine phalloidin staining of *wsh3.Δ* cells in which expression of the indicated *wsh3* allele was induced from a *leu1::nmt41wsh3.X* transgene (IH5737, 5738, 5739) by removal of thiamine for 24 hours. Bars, 5 μm.

induced excessive F-actin filaments, expression of *wsh3.V223A* or *wsh3.F225A* did not.

We conclude that the docking of PP1 to Wsh3/Tea4 is not required for the recruitment of either Wsh3/Tea4 or Tea1 to cell tips. It is, however, critically important for the role played by Wsh3/Tea4 in maintaining polarised tip growth as cells transit the cell cycle or recover from osmotic stress. This function is likely to involve modulation of the F-actin cytoskeleton as the ability of Wsh3/Tea4 to promote F-actin polymerisation is compromised when it cannot bind PP1.

Discussion

Tracking Dis2-NEGFP and Sds21-NEGFP fusion proteins enabled us to identify processes that are likely to be regulated by these PP1 holoenzymes. We extend the investigation by Ohkura et al. in which immunofluorescence with antibodies that recognised both Dis2 and Sds21 highlighted an enrichment in the nucleus in general and, in particular, the nucleolar region (Ohkura et al., 1989). The lack of a fixation step and the enhanced sensitivity of modern live cell imaging technologies, identified new locations at the cell tip, centromeres and endocytic vesicles, and a distinction between the distribution of Sds21 and Dis2.

Whereas the predicted amino acid sequences of Dis2 and Sds21 are strikingly similar [79% identical (Ohkura et al., 1989)], their distributions are significantly different. Dis2 was found at significant levels at a variety of locations including the entire nucleus, whereas Sds21 was found to accumulate in the nucleolus. Deleting *dis2*$^{+}$ enhanced Sds21 levels and Sds21 was then found at all the locations previously occupied by Dis2 with the exception of any enhancement of association with chromatin and the central dots seen prior to cytokinesis. However, it is important to note that these elevated levels of Sds21 were still below those of Dis2 (Ohkura et al., 1989) (see supplementary material Fig. S2). One interpretation is that free Sds21 has a limited half-life and yet is stabilised when bound to targeting sub-units, however, Dis2 has a greater affinity for many of these targeting sub-units so that the reduced affinity of Sds21 for these sub-units is reflected in reduced protein levels. The most important distinctions between the two molecules lie in their nuclear distribution as, at the crude level of detection signals, they do not appear to substitute for one another at these sites. This suggests that the actions at these sites might not be essential functions, but clearly demonstrates that the minor sequence divergence is functionally highly significant.

Such distinctions echo the fact that Dis2 contributes the majority of PP1 activity (Kinoshita et al., 1990) and a number of functional distinctions between Sds21 and Dis2. Enhanced Sds21 levels arrest cell cycle progression in G2 whereas elevating Dis2 protein do not (Yamano et al., 1994). This divergence in function was attributed to the ability of Dis2 to be downregulated by phosphorylation on a Cdc2 cyclin B phosphorylation site, T316, as overexpression of a *dis2.T316A* mutant provoked a G2 arrest (Ishii et al., 1996; Yamano et al., 1994). However, T316 does not appear to be essential for Dis2 function as a multi-copy plasmid expressing a version of *dis2* that lacks the last 30 amino acids (297-327) can support growth of *dis2.Δ sds21.Δ* cells (Kinoshita et al., 1991). A further distinction between Dis2 and Sds21 is illustrated by the unique role played by Dis2 in promoting recovery from DNA damage checkpoint arrest (den Elzen and O'Connell, 2004).

PP1 distribution in *S. pombe* is reminiscent of PP1 distribution in other systems. GFP fusion protein versions of the highly related α β δ and γ PP1 catalytic sub-unit isoforms of human cells have distinct distributions and show preferential recruitment to specific nuclear compartments. Whereas PP1α is excluded from the nucleolus in a diffuse nuclear pool, PP1β and PP1δ are equally distributed between the chromatin and nucleolus, but do not accumulate within the nucleoli to the same degree as PP1γ (Trinkle-Mulcahy et al., 2001). In addition, immunolocalisation data suggest that PP1α associates with centrosomes, PP1γ with the mitotic spindle and PP1δ with mitotic chromosomes (Andreassen et al., 1998; Fernandez et al., 1992). The single PP1 isoforms of *A. nidulans* and *S. cerevisiae*, BimG and Glc7, respectively, also accumulate in nuclei. Glc7 is permanently enriched in the nucleolus whereas BimG is a general nuclear protein in rich conditions, but accumulates in nucleoli during growth on a poor carbon source (Bloecher and Tatchell, 2000; Fox et al., 2002). As in *S. pombe*, discrete Glc7 spots co-localise with proteins associated with centromeres at the apex of anaphase nuclei (Bloecher and Tatchell, 2000). A discrete BimG dot mirrors the behaviour of centromeric Dis2 in associating with the SPB region throughout the cell cycle with the exception of the period when centromeres leave the SPB from mitotic entry until anaphase (Fox et al., 2002; Funabiki et al., 1993). However, it remains to be established whether this distribution arises from the association of PP1 with centromeres. Association of Glc7 with a kinetochore component is consistent with its role in counteracting the aurora kinase Ipl1 in the generation of unattached chromosomes to initiate the spindle checkpoint response (Francisco and Chan, 1994; Francisco et al., 1994; Hsu et al., 2000; Pinsky et al., 2006; Sassoon et al., 1999; Zhang et al., 2005). This role is likely to be conserved as human PP1γ shows a highly dynamic association with kinetochores either side of a more centrally located aurora B (Trinkle-Mulcahy et al., 2003), and levels of *ark1*$^{+}$ expression that do not kill wild-type cells (Petersen and Hagan, 2003) are fatal when *dis2* function is compromised (our unpublished data).

The cortical associations of Dis2 also echo data from the other fungi. Both Glc7 and BimG accumulate around the cytokinetic ring, the tips of growing hyphae or buds and sites from which hyphae will branch, or buds will emerge, respectively (Bloecher and Tatchell, 2000; Fox et al., 2002). Cortical PP1 has been studied in greatest detail in budding yeast, but it is clear that BimG is required for polarised growth during sporulation and vegetative growth (Doonan and Morris, 1989b; Fox et al., 2002).

The extensive characterisation of endocytosis in *S. cerevisiae* provides a framework within which to view Dis2 association with endocytic vesicles (Kaksonen et al., 2003; Kaksonen et al., 2005; Kaksonen et al., 2006). The motility of fusions between endocytic proteins and fluorescent proteins such as GFP defines three distinct phases in the endocytic vesicle cycle (Kaksonen et al., 2003; Kaksonen et al., 2005; Kaksonen et al., 2006). The site of endocytosis is determined in a non-motile phase by the co-operative action of molecules such as clathrin, Sla1, Sla2 and Pan1. The association of these proteins with the emerging vesicle persists through the next, slow motile, phase during

which the recruitment of myosin 5 and polymerisation of actin accompanies the formation of the clathrin pit. The vesicle then enters a rapid motile phase following the cessation of further actin polymerisation, the departure of myosin 5 and the scission of the pit to form the vesicle. Actin polymerisation is accompanied by the recruitment of homologues of the higher eukaryotic proteins N-WASP and the Arp2/3 complex, which harness actin polymerisation to promote scission and the eventual long range, fast motility of the free vesicle in the final phase (Kaksonen et al., 2003; Kaksonen et al., 2005; Kaksonen et al., 2006).

Glc7 regulates endocytosis via its association with the endocytic molecule Scd5 (Chang et al., 2002; Henry et al., 2002). Scd5 shuttles between the cytoplasm and the nucleus, associates with other endocytic proteins, Sla2 and Rvs167 and is required to maintain a wild-type actin cytoskeleton and for efficient endocytosis (Chang et al., 2006; Chang et al., 2002; Henry et al., 2002; Henry et al., 2003). Scd5 binds to Glc7 via a classic PP1 binding motif. Mutation of this motif compromise endocytosis, actin structure and confers temperature sensitive lethality (Chang et al., 2002). The suppression of *scd5* mutant phenotypes following deletion of the gene encoding the endocytic kinase Prk1 combines with biochemical data to suggest that Prk1 negatively regulates Scd5 (Henry et al., 2003), leading, in turn, to the proposal that following recruitment by Scd5 the Glc7-Scd5 holoenzyme counteracts Prk1 phosphorylation (Chang et al., 2006; Henry et al., 2003). As Prk1 phosphorylation acts at multiple levels to regulate actin dynamics and the association of endocytic proteins (Henry et al., 2003; Huang et al., 2003; Kaksonen et al., 2006; Sekiya-Kawasaki et al., 2003; Zeng and Cai, 1999; Zeng et al., 2001) a dynamic interplay between Scd5-Glc7 and Prk1 is likely to be critical to control endocytosis.

Although endocytosis is less extensively characterised in fission yeast, where it has been studied it mirrors that of budding yeast (Castagnetti et al., 2005; Ge et al., 2005; Sirotkin et al., 2005). The fission yeast Sla2 (also known as End4) protein localises in an identical manner to its budding yeast orthologue and is similarly required for endocytosis (Iwaki et al., 2004). By analogy with the three phases in budding yeast (Kaksonen et al., 2006), we found that Dis2 associates with vesicles during the non-motile phase and leaves just prior to the highly motile one. It was recruited to the patches after Sla2/End4. *S. cerevisiae* Sla2 physically binds to Scd5 and its recruitment to patches requires Scd5 (Chang et al., 2002; Henry et al., 2002). If conserved in *S. pombe* this relationship suggests that Scd5 first recruits Sla2/End4 and then Dis2 to the forming patches. As has been previously reported for Sla2/End4, depolymerisation of actin with Lat A did not block recruitment of Dis2 to the cell cortex but did freeze Dis2.NEGFP foci at the cell cortex before internalisation (Castagnetti et al., 2005; Ge et al., 2005; Sirotkin et al., 2005). In contrast to Wsp1 and Vrp1 (Sirotkin et al., 2005), neither Dis2 nor Sla2 formed aggregates at cell tips following actin depolymerisation, indicating that recruitment of Wsp1 and Vrp1 but not Dis2 or Sla2 depends upon actin dynamics. It is currently unclear whether the polarisation of endocytosis between growing tips and the nucleus (Castagnetti et al., 2005; Ge et al., 2005) is a secondary consequence of underlying growth polarity or is actively controlled to confer some advantage upon the cell.

The recruitment of a second population of Dis2.NEGFP foci to cell tips by Wsh3/Tea4 in a manner that is dependent upon the Kelch domain protein Tea1 (Martin et al., 2005; Tatebe et al., 2005) is highly reminiscent of budding yeast where Bud14 protein relies upon the Kelch domain proteins Kel1 and Kel2 to recruit Glc7 to the bud tip to control dynein activity during spindle orientation (Knaus et al., 2005). The *S. pombe* Bud14 homologue, Wsh3/Tea4 (Martin et al., 2005; Tatebe et al., 2005), both co-localised with Dis2 and physically associated with it. This association relied upon the conserved PP1 binding consensus site in Wsh3/Tea4. Mutation of this sequence blocked the recruitment of Dis2, but neither Tea1 nor Wsh3/Tea4 itself to cell tips.

Mutation of the PP1 binding sites in Wsh3/Tea4 compromised the control over the establishment and choice of polarised tip growth that accompanies cell cycle progression of unperturbed cultures and led to a major deficiency in re-establishing polarised growth from existing tips following osmotic stress. This function may be due, in part, to the impact of Wsh3/Tea4 upon actin polymerisation as the ability of excess Wsh3/Tea4 to induce excessive F-actin cables was abolished by mutation of the PP1 binding sites.

Thus, like its *A. nidulans* homologue BimG, Dis2 function is required for tip growth (Doonan and Morris, 1989; Fox et al., 2002). The requirement for PP1 function during recovery from stress, echoes the requirement for phosphorylation of the polo kinase Plo1 on serine 402 to promote tip growth during recovery from centrifugation and heat stress (Petersen and Hagan, 2005). However, it remains to be established whether Dis2 counteracts the action of polo kinase or any of the other protein kinases, such as Pom1, Kin1, Pck1 and Pck2 that modulate cell morphogenesis in fission yeast (Bähler and Pringle, 1998; Drewes and Nurse, 2003; La Carbona et al., 2004; Toda et al., 1993). Alternatively, it could play a critical role in modulating the activity of the kinases of the stress response pathway that associate with Wsh3/Tea4 (Tatebe et al., 2005). In this scenario the impact on morphogenesis would be mediated by stress signalling to either halt growth in the initial response to the stress, or to re-initiate it once cell composition has been changed to deal with this altered state (Petersen and Hagan, 2005).

Although Bud14 or Glc7 is required for spindle orientation rather than cell morphogenesis (Knaus et al., 2005), the conservation of Bud14-related molecules across species indicates that the identification of the substrates of the Dis2-Wsh3/Tea4 holoenzyme and clarifying its relationship with the cell polarity and morphogenesis kinases will shed much light on the control of the microtubule cytoskeleton and cell morphogenesis by protein phosphorylation in eukaryotes in general.

Materials and Methods

Strains, cell culture and molecular biology

Strains are listed in supplementary material Table S1. Standard fission yeast and molecular biology approaches were used throughout (Moreno et al., 1991). For imaging, cells were grown overnight in filter sterilised, appropriately supplemented, EMM2 (EMM2-FS) to mid log phase and mounted in a Bioptechs FC2 chamber with lectin (Sigma, L2380; 0.5 mg/ml). TRITC-labelled lectin (Sigma L5264) was used to preferentially label one strain in fields containing two strains (May and Mitchison, 1986). Latrunculin A (Lat A; Calbiochem 4280) and carbendazim (CBZ; Sigma PS1077) were dissolved in DMSO to generate stock solutions of 10 mM and 5 mg/ml, respectively.

Vectors to enable the C-terminal tagging of native loci with the fluorescent

proteins tdTomato and Cherry integration of PCR fragments were gifts from Kayoko Tanaka (University of Leicester, UK) and Michael Knop (EMBL, Heidelberg, Germany). The marker switch approach of MacIver et al. (MacIver et al., 2003a) in which the *ura4*$^+$ marker was inserted 266 and 640 bp upstream of the *dis2*$^+$ or *sds21*$^+$ ATG, respectively, was used to generate fusions in which the 3 Pk or EGFP tags from pGEM.Pk and pGEM.EGFP (Craven et al., 1998) were inserted at the initiator methionine codon after it had been mutated to introduce an *Nde*I site followed by sequences encoding three alanine residues immediately after the initiator methionine. Fragments that encompassed the sequences 435 and 70 bp upstream and 220 and 710 bp downstream of the Dis2 and Sds21 ORFs, respectively, were used for integration. After colony PCR confirmed that the tag had been successfully introduced, two rounds of backcrossing were undertaken. Deletion of *wsh3*$^+$ with *nat* was carried out according to the method of Hentges (Hentges et al., 2005).

Cell biology

A Perkin Elmer Ultraview spinning disk confocal head on a Zeiss Axiovert 200 or Deltavision Spectris system were used. Spinning disk images for Fig. 1A,C, Fig. 2A,B, Fig. 4, Fig. 5D,E, Figs 6, 7 and 8, and Movies 2-4 were captured as sets of 10-12×0.4 μm slices with a 20-second delay and the z series was compressed to a maximal projection. Images for Fig. 1B, Fig. 2C,D, Fig. 3, Fig. 5B,C,F, Figs 9, 10, supplementary material Fig. S1, Fig. S2B, Fig. S3A, Fig. S4 were captured with the Deltavision Spectris system. One focal plane snapshots were captured for Fig. 1B, Fig. 3. Images for Fig. 2C,D, Fig. 10F and supplementary material Fig. S2B were captured as sets of 20×0.3 μm slices whereas images and the z series were compressed to give the images in the panels. Images for Fig. 9, Fig. 10B, and supplementary material Fig. S3A, Fig. S4 were captured as sets of 3×0.3 μm slices and the z series was compressed to a maximal projection. To study DEAF movement, one single focal plane was captured continuously, without delay between time points, for 100-300 seconds with the spinning disk for Fig. 5A and Movie 1 and with the Deltavision Spectris system for Fig. 5B,C,F. All image analysis used Imaris (Bitplane) software. The stage and phase turret of the axiovert 200 microscope were encapsulated in a heated Perspex environmental chamber (Solent scientific, Segensworth, UK) and the Zeiss 100× 1.45 NA α plan-FLUAR lens was fitted with a Bioptecs objective heater. To inactivate temperature-sensitive gene products, the chamber, objective heater and Bioptechs coverglass were all heated to 33°C or 36°C.

Biochemistry

Standard western blotting approaches following TCA precipitation were as described previously (MacIver et al., 2003b). For western blotting, immunofluorescence and immunoprecipitation α-V5 (bethyl A190-120A), α-GFP polyclonal antibodies were used. Chromatin immunoprecipitation PCR utilised the procedures and primers outlined by Pidoux et al. (Pidoux et al., 2004).

We would like to thank Tony Carr, Roger Tsien, Kayoko Tanaka, Takashi Toda, Elmar Schiebel, Paul Nurse, Stephania Castagnetti, Fred Chang, Michael Knop and Kathryn Ayscough for strains and reagents, and Steve Bagley for support in the Advanced Imaging Facility in the Paterson Institute. We are particularly indebted to Alison Pidoux and Wolfgang Reiter for advice on ChIP procedures. This work was supported by Cancer Research UK [CRUK] and the Basque Government.

References

Andreassen, P. R., Lacroix, F. B., Villa-Moruzzi, E. and Margolis, R. L. (1998). Differential subcellular localization of protein phosphatase-1 alpha, gamma1, and delta isoforms during both interphase and mitosis in mammalian cells. *J. Cell Biol.* **141**, 1207-1215.

Arellano, M., Niccoli, T. and Nurse, P. (2002). Tea3p is a cell end marker activating polarized growth in Schizosaccharomyces pombe. *Curr. Biol.* **12**, 751-756.

Bähler, J. and Pringle, J. R. (1998). Pom1p, a fission yeast protein kinase that provides positional information for both polarized growth and cytokinesis. *Genes Dev.* **12**, 1356-1370.

Beinhauer, J. D., Hagan, I. M., Hegemann, J. H. and Fleig, U. (1997). Mal3, the fission yeast homolog of the human APC-interacting protein EB-1 is required for microtubule integrity and the maintenance of cell form. *J. Cell Biol.* **139**, 717-728.

Bloecher, A. and Tatchell, K. (2000). Dynamic localization of protein phosphatase type 1 in the mitotic cell cycle of *Saccharomyces cerevisiae*. *J. Cell Biol.* **149**, 125-140.

Browning, H., Hayles, J., Aveline, L., Nurse, P. and McIntosh, J. R. (1998). A kinesin-like protein required for proper cellular morphology in *Schizosaccharomyces pombe*. *Mol. Biol. Cell* **9**, 2275.

Browning, H., Hayles, J., Mata, J., Aveline, L., Nurse, P. and McIntosh, J. R. (2000). Tea2p is a kinesin-like protein required to generate polarized growth in fission yeast. *J. Cell Biol.* **151**, 15-28.

Browning, H., Hackney, D. D. and Nurse, P. (2003). Targeted movement of cell end factors in fission yeast. *Nat. Cell Biol.* **5**, 812-818.

Brunner, D. and Nurse, P. (2000). CLIP170-like tip1 spatially organizes microtubular dyanmics in fission yeast. *Cell* **102**, 695-704.

Busch, K. E. and Brunner, D. (2004). The microtubule plus end-tracking proteins mal3p and tip1p cooperate for cell-end targeting of interphase microtubules. *Curr. Biol.* **14**, 548-559.

Castagnetti, S., Behrens, R. and Nurse, P. (2005). End4/Sla2 is involved in establishment of a new growth zone in *Schizosaccharomyces pombe*. *J. Cell Sci.* **118**, 1843-1850.

Ceulemans, H. and Bollen, M. (2004). Functional diversity of protein phosphatase-1, a cellular economizer and reset button. *Physiol. Rev.* **84**, 1-39.

Ceulemans, H., Stalmans, W. and Bollen, M. (2002). Regulator-driven functional diversification of protein phosphatase-1 in eukaryotic evolution. *BioEssays* **24**, 371-381.

Chang, J. S., Henry, K., Wolf, B. L., Geli, M. and Lemmon, S. K. (2002). Protein phosphatase-1 binding to scd5p is important for regulation of actin organization and endocytosis in yeast. *J. Biol. Chem.* **277**, 48002-48008.

Chang, J. S., Henry, K., Geli, M. I. and Lemmon, S. K. (2006). Cortical recruitment and nuclear-cytoplasmic shuttling of Scd5p, a protein phosphatase-1-targeting protein involved in actin organization and endocytosis. *Mol. Biol. Cell* **17**, 251-262.

Craven, R. A., Griffiths, D. J. F., Sheldrick, K. S., Randall, R. E., Hagan, I. M. and Carr, A. M. (1998). Vectors for the expression of tagged proteins in *Schizosaccharomyces pombe. Gene* **221**, 59-68.

den Elzen, N. R. and O'Connell, M. J. (2004). Recovery from DNA damage checkpoint arrest by PP1-mediated inhibition of Chk1. *EMBO J.* **23**, 908-918.

Doonan, J. H. and Morris, N. R. (1989). The *bimG* gene of *Aspergillus nidulans*, required for completion of anaphase, encodes a homolog of mammalian phosphoprotein phosphatase 1. *Cell* **57**, 987-996.

Drewes, G. and Nurse, P. (2003). The protein kinase kin1, the fission yeast orthologue of mammalian MARK/PAR-1, localises to new cell ends after mitosis and is important for bipolar growth. *FEBS Lett.* **554**, 45-49.

Feierbach, B. and Chang, F. (2001). Roles of the fission yeast formin for3p in cell polarity, actin cable formation and symmetric cell division. *Curr. Biol.* **11**, 1656-1665.

Feierbach, B., Verde, F. and Chang, F. (2004). Regulation of a formin complex by the microtubule plus end protein tea1p. *J. Cell Biol.* **165**, 697-707.

Fernandez, A., Brautigan, D. L. and Lamb, N. J. (1992). Protein phosphatase type 1 in mammalian cell mitosis: chromosomal localization and involvement in mitotic exit. *J. Cell Biol.* **116**, 1421-1430.

Fox, H., Hickey, P. C., Fernandez-Abalos, J. M., Lunness, P., Read, N. D. and Doonan, J. H. (2002). Dynamic distribution of BIMG(PP1) in living hyphae of Aspergillus indicates a novel role in septum formation. *Mol. Microbiol.* **45**, 1219-1230.

Francisco, L. and Chan, C. S. M. (1994). Regulation of yeast chromosome segregation by Ipl1 protein-kinase and type-1 protein phosphatase. *Cell. Mol. Biol. Res.* **40**, 207-213.

Francisco, L., Wang, W. F. and Chan, C. S. M. (1994). Type-1 protein phosphatase acts in opposition to Ipl1 protein-kinase in regulating yeast chromosome segregation. *Mol. Cell. Biol.* **14**, 4731-4740.

Funabiki, H., Hagan, I., Uzawa, S. and Yanagida, M. (1993). Cell cycle-dependent specific positioning and clustering of centromeres and telomeres in fission yeast. *J. Cell Biol.* **121**, 961-976.

Garcia, M. A., Vardy, L., Koonrugsa, N. and Toda, T. (2001). Fission yeast ch-TOG/XMAP215 homologue Alp14 connects mitotic spindles with the kinetochore and is a component of the Mad2-dependent spindle checkpoint. *EMBO J.* **20**, 3389-3401.

Ge, W., Chew, T. G., Wachtler, V., Naqvi, S. N. and Balasubramanian, M. K. (2005). The novel fission yeast protein Pal1p interacts with Hip1-related Sla2p/End4p and is involved in cellular morphogenesis. *Mol. Biol. Cell* **16**, 4124-4138.

Glynn, J. M., Lustig, R. J., Berlin, A. and Chang, F. (2001). Role of bud6p and tea1p in the interaction between actin and microtubules for the establishment of cell polarity in fission yeast. *Curr. Biol.* **11**, 836-845.

Grallert, A., Beuter, C., Craven, R. A., Bagley, S., Wilks, D., Fleig, U. and Hagan, I. M. (2006). *S. pombe* CLASP needs dynein, not EB1 or CLIP170, to induce microtubule instability and slows polymerization rates at cell tips in a dynein-dependent manner. *Genes Dev.* **20**, 2421-2436.

Hagan, I. M. (1998). Fission yeast microtubules. *J. Cell Sci.* **111**, 1603-1612.

Hagan, I. and Yanagida, M. (1997). Evidence for cell cycle-specific, spindle pole body-mediated, nuclear positioning in the fission yeast *Schizosaccharomyces pombe*. *J. Cell Sci.* **110**, 1851-1866.

Hayles, J. and Nurse, P. (2001). A journey into space. *Nat. Rev. Mol. Cell Biol.* **2**, 647-656.

Henry, K. R., D'Hondt, K., Chang, J., Newpher, T., Huang, K., Hudson, R. T., Riezman, H. and Lemmon, S. K. (2002). Scd5p and clathrin function are important for cortical actin organization, endocytosis, and localization of sla2p in yeast. *Mol. Biol. Cell* **13**, 2607-2625.

Henry, K. R., D'Hondt, K., Chang, J. S., Nix, D. A., Cope, M. J., Chan, C. S., Drubin, D. G. and Lemmon, S. K. (2003). The actin-regulating kinase Prk1p negatively regulates Scd5p, a suppressor of clathrin deficiency, in actin organization and endocytosis. *Curr. Biol.* **13**, 1564-1569.

Hentges, P., Van Driessche, B., Tafforeau, L., Vandenhaute, J. and Carr, A. M. (2005). Three novel antibiotic marker cassettes for gene disruption and marker switching in *Schizosaccharomyces pombe*. *Yeast* **22**, 1013-1019.

Hsu, J.-Y., Sun, Z.-W., Li, X., Reuben, M., Tatchell, K., Bishop, D. K., Grushcow, J. M., Brame, C. J., Caldwell, J. A., Hunt, D. F. et al. (2000). Mitotic phosphorylation of Histone H3 is governed by Ilp1/aurora kinase and Glc7/PP1 phosphatase in budding yeast and nematodes. *Cell* **102**, 279-291.

Huang, B., Zeng, G., Ng, A. Y. and Cai, M. (2003). Identification of novel recognition motifs and regulatory targets for the yeast actin-regulating kinase Prk1p. *Mol. Biol. Cell* **14**, 4871-4884.

Ingebritsen, T. S. and Cohen, P. (1983). Protein phosphatases: properties and role in cellular regulation. *Science* **221**, 331-338.

Ishii, K., Kumada, K., Toda, T. and Yanagida, M. (1996). Requirement for PP1 phosphatase and 20S cyclosome/APC for the onset of anaphase is lessened by the dosage increase of a novel gene sds23^{+}. *EMBO J.* **15**, 6629-6640.

Iwaki, T., Tanaka, N., Takagi, H., Giga-Hama, Y. and Takegawa, K. (2004). Characterization of *end4*$^{+}$, a gene required for endocytosis in *Schizosaccharomyces pombe*. *Yeast* **21**, 867-881.

Kaksonen, M., Sun, Y. and Drubin, D. G. (2003). A pathway for association of receptors, adaptors, and actin during endocytic internalization. *Cell* **115**, 475-487.

Kaksonen, M., Toret, C. P. and Drubin, D. G. (2005). A modular design for the clathrin- and actin-mediated endocytosis machinery. *Cell* **123**, 305-320.

Kaksonen, M., Toret, C. P. and Drubin, D. G. (2006). Harnessing actin dynamics for clathrin-mediated endocytosis. *Nat. Rev. Mol. Cell Biol.* **7**, 404-414.

Kinoshita, N., Ohkura, H. and Yanagida, M. (1990). Distinct, essential roles of Type-1 and Type-2a protein phosphatases in the control of the fission yeast-cell division cycle. *Cell* **63**, 405-415.

Kinoshita, N., Yamano, H., Lebouffantsladeczek, F., Kurooka, H., Ohkura, H., Stone, E. M., Takeuchi, M., Toda, T., Yoshida, T. and Yanagida, M. (1991). Sister-chromatid separation and protein dephosphorylation in mitosis. *Cold Spring Harb. Symp. Quant. Biol.* **56**, 621-628.

Knaus, M., Cameroni, E., Pedruzzi, I., Tatchell, K., De Virgilio, C. and Peter, M. (2005). The Bud14p-Glc7p complex functions as a cortical regulator of dynein in budding yeast. *EMBO J.* **24**, 3000-3011.

La Carbona, S., Allix, C., Philippe, M. and Le Goff, X. (2004). The protein kinase kin1 is required for cellular symmetry in fission yeast. *Biol. Cell* **96**, 169-179.

MacIver, F. H., Glover, D. M. and Hagan, I. M. (2003a). A 'marker switch' approach for targeted mutagenesis of genes in *Schizosaccharomyces pombe*. *Yeast* **20**, 587-594.

MacIver, F. H., Tanaka, K., Robertson, A. M. and Hagan, I. M. (2003b). Physical and functional interactions between polo kinase and the spindle pole component Cut12 regulate mitotic commitment in *S. pombe*. *Genes Dev.* **17**, 1507-1523.

Manning, G., Plowman, G. D., Hunter, T. and Sudarsanam, S. (2002). Evolution of protein kinase signaling from yeast to man. *Trends Biochem. Sci.* **27**, 514-520.

Marks, J. and Hyams, J. S. (1985). Localization of F-actin through the cell-division cycle of *Schizosaccharomyces pombe*. *Eur. J. Cell Biol.* **39**, 27-32.

Martin, S. G., McDonald, W. H., Yates, J. R., 3rd and Chang, F. (2005). Tea4p links microtubule plus ends with the formin for3p in the establishment of cell polarity. *Dev. Cell* **8**, 479-491.

Mata, J. and Nurse, P. (1997). Tea1 and the microtubular cytoskeleton are important for generating global spatial order within the fission yeast cell. *Cell* **89**, 939-949.

May, J. and Mitchison, J. M. (1986). Length growth in fission yeast cells measured by two novel techniques. *Nature* **322**, 752-754.

Meiselbach, H., Sticht, H. and Enz, R. (2006). Structural analysis of the protein phosphatase 1 docking motif: molecular description of binding specificities identifies interacting proteins. *Chem. Biol.* **13**, 49-59.

Mitchison, J. M. and Nurse, P. (1985). Growth in cell length in the fission yeast *Schizosaccharomyces pombe*. *J. Cell Sci* **75**, 357-376.

Moreno, S., Klar, A. and Nurse, P. (1991). Molecular genetic analysis of fission yeast *Schizosaccharomyces pombe*. *Meth. Enzymol.* **194**, 795-823.

Ohkura, H., Kinoshita, N., Miyatani, S., Toda, T. and Yanagida, M. (1989). The fission yeast *dis2*$^{+}$ gene required for chromosome disjoining encodes one of two putative type-1 protein phosphatases. *Cell* **57**, 997-1007.

Pelham, R. J., Jr and Chang, F. (2001). Role of actin polymerization and actin cables in actin-patch movement in *Schizosaccharomyces pombe*. *Nat. Cell Biol.* **3**, 235-244.

Petersen, J. and Hagan, I. M. (2003). *S. pombe* aurora kinase/survivin is required for chromosome condensation and the spindle checkpoint attachment response. *Curr. Biol.* **30**, 590-597.

Petersen, J. and Hagan, I. M. (2005). Polo kinase links the stress pathway to cell cycle control and tip growth in fission yeast. *Nature* **435**, 507-512.

Pidoux, A., Mellone, B. and Allshire, R. (2004). Analysis of chromatin in fission yeast. *Methods* **33**, 252-259.

Pinsky, B. A., Kotwaliwale, C. V., Tatsutani, S. Y., Breed, C. A. and Biggins, S. (2006). Glc7/protein phosphatase 1 regulatory subunits can oppose the Ipl1/aurora protein kinase by redistributing Glc7. *Mol. Cell. Biol.* **26**, 2648-2660.

Ptacek, J., Devgan, G., Michaud, G., Zhu, H., Zhu, X., Fasolo, J., Guo, H., Jona, G., Breitkreutz, A., Sopko, R. et al. (2005). Global analysis of protein phosphorylation in yeast. *Nature* **438**, 679-684.

Saitoh, S., Takahashi, K. and Yanagida, M. (1997). Mis6, a fission yeast inner centromere protein, acts during G1/S and forms specialized chromatin required for equal segregation. *Cell* **90**, 131-143.

Sassoon, I., Severin, F., Andrews, P. D., Taba, M.-R., Kaplan, K. B., Ashford, A. J., Stark, M. J. R., Sorger, P. K. and Hyman, A. A. (1999). Regulation of *Saccharomyces cerevisiae* kinetochores by the type 1 phosphatase Glc7p. *Genes Dev.* **13**, 545-555.

Sekiya-Kawasaki, M., Groen, A. C., Cope, M. J., Kaksonen, M., Watson, H. A., Zhang, C., Shokat, K. M., Wendland, B., McDonald, K. L., McCaffery, J. M. et al. (2003). Dynamic phosphoregulation of the cortical actin cytoskeleton and endocytic machinery revealed by real-time chemical genetic analysis. *J. Cell Biol.* **162**, 765-772.

Shaner, N. C., Campbell, R. E., Steinbach, P. A., Giepmans, B. N., Palmer, A. E. and Tsien, R. Y. (2004). Improved monomeric red, orange and yellow fluorescent proteins derived from *Discosoma sp.* red fluorescent protein. *Nat. Biotechnol.* **22**, 1567-1572.

Sirotkin, V., Beltzner, C. C., Marchand, J. B. and Pollard, T. D. (2005). Interactions of WASp, myosin-I, and verprolin with Arp2/3 complex during actin patch assembly in fission yeast. *J. Cell Biol.* **170**, 637-648.

Snaith, H. A. and Sawin, K. E. (2003). Fission yeast mod5p regulates polarized growth through anchoring of tea1p at cell tips. *Nature* **423**, 647-651.

Stark, M. J. R. (1996). Yeast protein serine/threonine phosphatases: multiple roles and diverse regulation. *Yeast* **12**, 1647-1675.

Takahashi, K., Chen, E. S. and Yanagida, M. (2000). Requirement of Mis6 centromere connector for localizing a CENP-A-like protein in fission yeast. *Science* **288**, 2215-2219.

Tatebe, H., Shimada, K., Uzawa, S., Morigasaki, S. and Shiozaki, K. (2005). Wsh3/Tea4 is a novel cell-end factor essential for bipolar distribution of tea1 and protects cell polarity under environmental stress in *S. pombe*. *Curr. Biol.* **15**, 1006-1015.

Toda, T., Yamamoto, M. and Yanagida, M. (1981). Sequential alterations in the nuclear chromatin region during mitosis of the fission yeast *Schizosaccharomyces pombe*: video fluorescence microscopy of synchronously growing wild-type and cold-sensitive *cdc* mutants by using a DNA-binding fluorescent-probe. *J. Cell Sci.* **52**, 271-287.

Toda, T., Shimanuki, M. and Yanagida, M. (1993). Two novel protein kinase C-related genes of fission yeast are essential for cell viability and implicated in cell shape control. *EMBO J.* **12**, 1987-1995.

Trinkle-Mulcahy, L., Sleeman, J. E. and Lamond, A. I. (2001). Dynamic targeting of protein phosphatase 1 within the nuclei of living mammalian cells. *J. Cell Sci.* **114**, 4219-4228.

Trinkle-Mulcahy, L., Andrews, P. D., Wickramasinghe, S., Sleeman, J., Prescott, A., Lam, Y. W., Lyon, C., Swedlow, J. R. and Lamond, A. I. (2003). Time-lapse imaging reveals dynamic relocalization of PP1gamma throughout the mammalian cell cycle. *Mol. Biol. Cell* **14**, 107-117.

Verde, F., Mata, J. and Nurse, P. (1995). Fission yeast-cell morphogenesis – identification of new genes and analysis of their role during the cell-cycle. *J. Cell Biol.* **131**, 1529-1538.

Yamano, H., Ishii, K. and Yanagida, M. (1994). Phosphorylation of Dis2 protein phosphatase at the C-terminal Cdc2 consensus and its potential role in cell-cycle regulation. *EMBO J.* **13**, 5310-5318.

Zeng, G. and Cai, M. (1999). Regulation of the actin cytoskeleton organization in yeast by a novel serine/threonine kinase Prk1p. *J. Cell Biol.* **144**, 71-82.

Zeng, G., Yu, X. and Cai, M. (2001). Regulation of yeast actin cytoskeleton-regulatory complex Pan1p/Sla1p/End3p by serine/threonine kinase Prk1p. *Mol. Biol. Cell* **12**, 3759-3772.

Zhang, K., Lin, W., Latham, J. A., Riefler, G. M., Schumacher, J. M., Chan, C., Tatchell, K., Hawke, D. H., Kobayashi, R. and Dent, S. Y. (2005). The Set1 methyltransferase opposes Ipl1 aurora kinase functions in chromosome segregation. *Cell* **122**, 723-734.